Colloid & Polymer Science Colloid Polym Sci 272: 293–300 (1994)

The solubility limit of a solid solutions for the systems of long-chain symmetrical ketones in an *n*-alkane matrix

K. Takamizawa, K. Nakasone, and Y. Urabe

Department of Applied Science, Faculty of Engineering, Kyushu University, Japan

Abstract: The systems of long-chain symmetrical ketones in *n*-alkane matrices form solid solutions for a low concentration range of the ketone, when the number of carbon atoms n in a ketone molecule Kn is equal to or lower than that in a *n*-alkane molecule. The Kn examined were K25 to K39. The purity of all the samples used was very high. The solubility limit of these solid solutions was determined with DSC measurements. Above the solubility limit (the critical concentration) the systems changed to eutectic mixtures. The relationships for the solubility limit were derived, taking into consideration the lateral two-dimensional and the longitudinal positioning along the chain axes and the correlating energies. The multiplicity of the longitudinal positioning led to a remarkable increase in the solubility limit of the systems of Kn/Cn′ ($n' > n$). The present result points to the importance of the entropy of mixing and also for the stability of long-chain crystals.

Key words: Symmetrical ketone – *n*-alkane – solubility limit – solid solution – entropy of mixing

Introduction

In order to obtain insight into the thermal behavior of polyethylene crystals, many works on the *n*-alkane crystals as a model compound have been performed. One of the thermal characteristics of higher *n*-alkane crystals is the polymorphic transition. A transition to the hexagonal phase has been widely known to occur for the *n*-alkanes whose number of carbon atoms in the molecule n is lower than about 40. Recently, other types of polymorphic transitions were observed for pure *n*-alkanes. In this transition the mode of the lateral packing of the chain molecules remains unchanged in the orthorhombic sub-cell [1–3]. Higher odd *n*-alkanes in general transform from the orthorhombic modification (abbreviated as A) to monoclinic (B) and the monoclinic form (C), in addition to the hexagonal transition [1, 2]. Higher even *n*-alkanes (n > 36) also show transitions similar to the C phase transition [2, 3]. Our preliminary study indicated that the high-temperature modification (C′) of even *n*-alkanes was also monoclinic, whereas the space group seemed to differ from odd *n*-alkanes [3, 4]. The structural feature of the C- and the C′-phases is that the end methyl plane inclines to the chain axes. The DSC curves for the solution-crystallized *n*-alkanes showed higher heat capacities over the C and C′ phases than those for the room-temperature modification and liquid [4]. Although the detailed origin of the phenomena is still unknown, the presence of longitudinal disorder in the C phase of tritriacontane was already reported [5]. To elucidate the intrinsic nature of these high-temperature modifications is important for the understanding of the molecular motion in the crystalline field, which may correlate with the defects in the chain crystals as well as the crystalline relaxation phenomena.

On the other hand, the molecular motion of long-chain polar molecules in a non-polar crystalline field has been studied with a dielectric relaxation technique [6–9]. Typical systems consisted

of symmetrical long ketone and *n*-alkane as a matrix, whose chain length was longer by one methylene unit than that of the ketone. In an alternating electric field the ketone molecules moved between two equilibrium positions with a "flip-flop" mechanism [9]. It seemed that both components form a substitutional mixture over the whole concentration range because the subcell lattice parameters of the ketones and the *n*-alkanes are nearly identical. However, two components showed partial solubility because of dipole dipole repulsion in the mixture. Meakins named the phase diagram of 12-tricosanone and hexacosane system a "eutectic of solid solution" [6].

n-Alkane mixtures make solid solutions when the differences between their chain lengths are small, but make eutectic mixtures when the differences are large. They do not show the critical concentration of solid solution, in contrast with the *n*-alkane-ketone mixtures [10]. It is interesting to learn how the solubility limit of the solid solution is determined by thermodynamics. This information may be useful for the understanding of the effect of homologous impurity of *n*-alkane crystals, as well as the nature of high-temperature modification of higher *n*-alkane crystals. This system may also become a model for poly(ethylene-*co*-carbon monoxide).

The purpose of the present paper is to establish the relationship between the solubility limit of the solid solution at a low concentration range of ketone and the chain length of both components. The phase diagrams were determined by DSC measurements and observations with the polarizing microscope. The solubility limit could be expressed in terms of the entropy of mixing.

Experimental

Samples

Four symmetrical ketones, 13-pentacosanone, 15-nonacosanone, 16-hentriacontanone, and 20-nonatriacontanone were used. They are abbreviated as K25, K29, K31, and K39, respectively, where the numeral is the number of the carbon atoms. The ketones were synthesized through a ketene dimerization reaction from the corresponding carbonic acid chlorides, which were free from other homologues. The details of the purification technique of starting materials and synthetic method were previously reported [11]. The ketones finally were purified with recrystallization and elution through a silica gel column. The odd *n*-alkanes, that is, pentacosane, heptacosane, nonacosane, hentriacontane, and nonatriacontane were synthesized by reducing corresponding ketones using the Wolff–Kishner method. Hexacosane and octacosane were purchased from Sigma Chemical Co. All the *n*-alkanes were purified by column elution after treatment with hot concentrated sulfuric acid. The *n*-alkanes are abbreviated as Cn.

Table1. Purity of symmetrtic long-chain ketones and *n*-alkanes

Samples	Purity/%
13-Pentacosanone (K25)	100.0
15-Nonacosanone (K29)	99.9
16-Hentriacontanone (K31)	99.9
20-Nonatriacontanone (K39)	99.7
Pentacosane (C25)	100.0
Hexacosane (C26)	99.8
Heptacosane (C27)	100.0
Octacosane (C28)	99.9
Nonacosane (C29)	99.9
Hentriacontane (C31)	99.9
Nonatriacontane (C39)	99.9

The sample purity was determined with a Shimadzu capillary gas chromatograph GC-14A, equipped with a column of CBP1-M25-025. The purities are listed in Table 1.

Measurements

DSC measurements were performed with a Rigaku DSC 8240B-TAS 100 system. The standard operational conditions were: sample weight of 1.500 ± 0.005 mg and a heating rate of 0.5 K/min. Two components were homogeneously mixed in a hexane or heptane solution. After drying under a vacuum, the mixture was crystallized with a cooling rate of 3 K/h from the melt. For the systems of K31/C31 and K39/C39, a cooling rate of 2K/h was adopted.

The polarizing microscopic measurements were done with a Nikon POH microscope equipped with a small heater. Its temperature

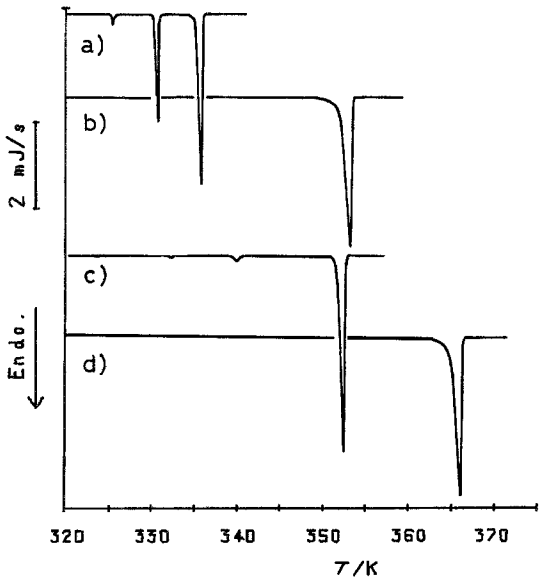

Fig. 1. DSC curves of pure *n*-alkanes and of pure symmetrical ketones, crystallized from the melt. Weight of sample: 1.50 mg, heating rate: 30 K/h. a) C29, b) K29, c) C39, and d) K39

was controlled within 0.04 K. Observations were done on samples covered with a cover glass.

The X-ray diffraction measurement was done with a Stoe diffractometer with Ni filtered CuKα radiation at a room temperature.

Results and discussion

Properties of pure components

DSC curves for K29 and K39, which were crystallized from the melt, are shown in Fig. 1. The cooling rates for K25 and K29 were 3 K/h and those for K31 and K39 were 2 K/h, respectively. DSC curves for bulk crystallized C29 and C39 are also shown in Fig. 1. The feature that the ketones melt without any indication of solid-solid transitions presents a remarkable contrast to that of *n*-alkanes. All melting points of Kn are higher than that of Cn. The crystal structures stable at room temperature are orthorhombic for odd Cn and monoclinic for even ones. As described in the Introduction, *n*-alkanes show complicated polymorphic transitions. Odd Cn shows the B phase transition for $n \geq 27$ and in addition to it the transition from the B to the C phase for $n \geq 33$.

Table 2. Lattice parameters of 13-pentacosanone (K25) and pentacosane (C25)

Lattice constant*)	K25	C25
a	740	745
b	501	496
c	3370	3380

*) In a unit of pm

The DSC curve for C39 in Fig. 1 clearly shows the B and the C solid-solid transitions. Although Broadhurst's compilation of the thermodynamic and structural data on *n*-alkanes indicated that C43 was the highest member which showed the hexagonal phase [12], the curve of C39 does not indicate the presence of this transition. As previously described, the even C26 and C28 show only the hexagonal transition before the melting.

Table 2 shows the lattice constants of K25 and C25. The length of the crystal axes for both are almost identical. It seems that lattice strains are not introduced into the mixtures of either component.

Theoretical consideration on the solubility limit in the low concentration region of ketones

As will be described later, when the chain length of the ketone is equal to or shorter than that of *n*-alkane matrix, the solid mixture over a low concentration range of the ketone may form a solid solution. It is reasonable to assume that layered crystals are formed. When both components have an identical chain length and the interactions between the constituent molecules are weak, the entropy of mixing of the system of Kn/Cn (where n is the number of carbon atoms in a molecule) in the zeroth approximation is given as

$$\Delta S = k\ln \{N_0!/[N!(N_0 - N)!]\} , \quad (1)$$

where N_0 is the total number of the two-dimensional lattice sites and N the number of Kn molecules. Random substitution of the Kn molecule in the Cn matrix, as schematically shown in Fig. 2-A, may lead to an increase in energy by $\Delta\varepsilon_0$ per Kn molecule. Strictly speaking, the value of $\Delta\varepsilon_0$ may depend on the concentration of ketones in the range of high concentration. However, we assume

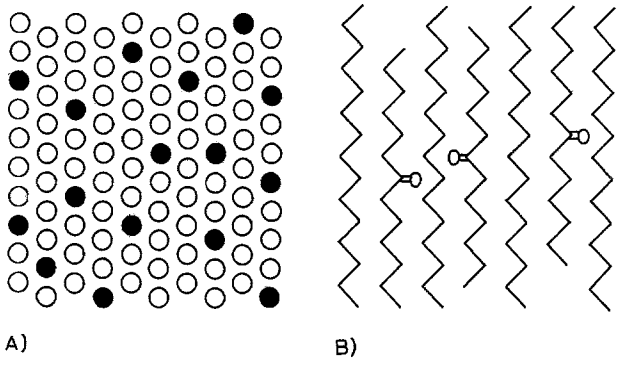

Fig. 2. Schematic positions of Kn in a Cn' matrix. A) Lateral position of Kn in a pseudohexagonal lattice. Filled circles indicate Kn. B) Longitudinal position of Kn in a matrix composed of longer Cn.

that $\Delta\varepsilon_0$ is an empirical parameter whose value is independent of the concentration of ketones in whole range studied. Minimizing the free energy with respect to N (N is taken as the order parameter in this method), the equilibrium concentration of Kn is estimated as

$$N/(N_0 - N) = \exp(-\Delta\varepsilon_0/kT) . \quad (2)$$

This corresponds to the critical concentration, c_C, of the solid solution, above which the mixture becomes eutectic. The disposition on the two-dimensional lattice, formed at a crystallization temperature T_C, does not change due to further cooling because of the difficulty in the exchange of long-chain molecules. The temperature in the exponent of Eq. (2) has to be read as T_C in the zeroth approximation. We could experimentally determine c_C as a boundary concentration between the solid solution and the eutectic mixture.

When Kn is shorter than the layer thickness of the matrix, Kn can be located on several equilibrium positions along the chain direction, as schematically shown in Fig. 2-B. Let the number of the disposition be m. With an assumption that the disposition in the two-dimensional lattice and that along the chain direction are independent, the entropy of mixing may be modified as

$$\Delta S = k\ln\{m\lambda N_0!/[N!(N_0 - N)!]\} . \quad (3)$$

And, also, a vacant energy has to be added because vacant sites are introduced at the chain-end parts of the matrix. Let the vacant energy per one site be $\Delta\varepsilon_v$. The equilibrium concentration may be

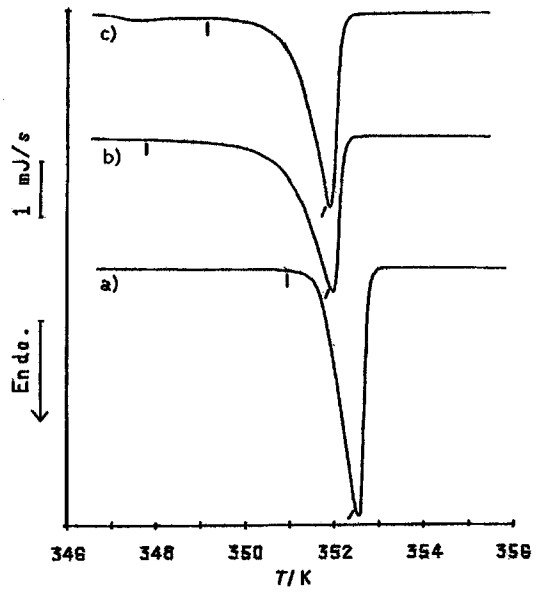

Fig. 3. DSC curves of pure C39 and mixtures with K39 in the range of concentration corresponding to the solid solution. The curves are represented on a magnified scale in temperature. Vertical and oblique bars indicate the temperatures of a solidus and liquidus lines, respectively. a) pure C39; b) 12.7; c) 22.6 mol% of K39.

represented by the following equation:

$$N/(N_0 - N) = m\exp(-\Delta\varepsilon_0/kT) \times \exp[-(m-1)\Delta\varepsilon_v/kT] . \quad (4)$$

Strictly speaking, it is possible that $\Delta\varepsilon^0$ for m > 1 may become somewhat smaller than that for $m = 1$. Due to the first factor of the right-hand side of Eq. (4), m, c_C may increase with an increase of the difference in the number of carbon atoms between the n-alkane and the ketone, Δn.

The critical concentration for the systems of Kn/Cn

As previously stated, C39 melts without the hexagonal transition. The DSC melting peak is simple and sharp. Figure 3 shows the melting peaks for the pure C39 and the mixtures of K39/C39 (concentration c below 22.6 mol%), on a magnified temperature scale. Even for the mixtures the peaks are simple, but become broader around 10 mol%. The temperature at which an extrapolated line of the DSC peak front intersects with a base line is usually defined as the melting

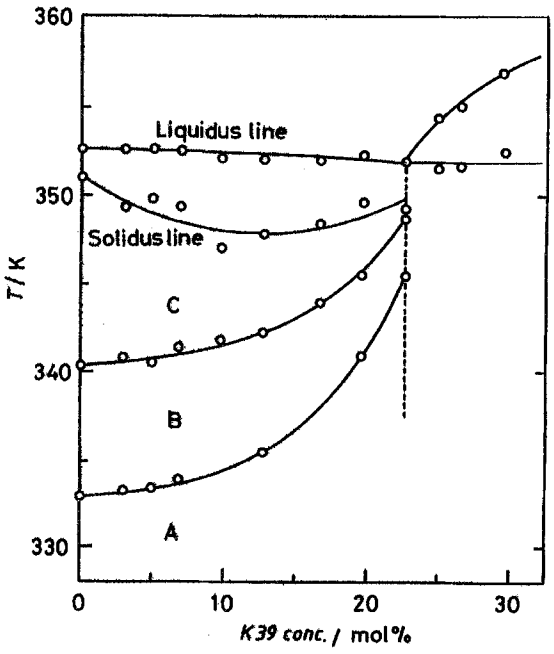

Fig. 4. Phase diagram of the system K39/C39 in a range of low concentration of K39. Up to about 22.6 mol% the system forms solid solution and above it is a eutectic mixture. Solidus and liquidus lines of the solid solution were estimated by the procedure described in the text

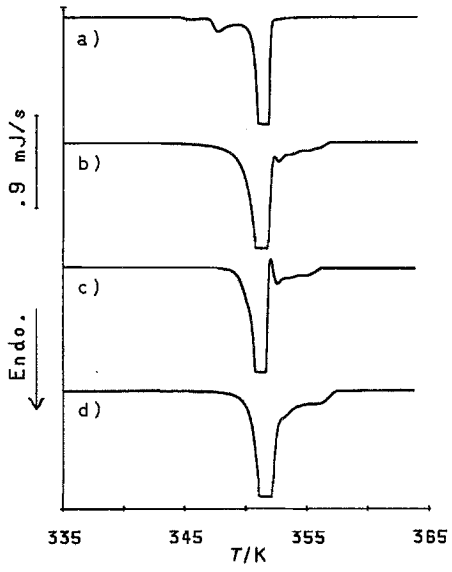

Fig. 5. DSC curves for mixtures of K39 in C39 in the critical concentration and above it. The ordinate scale is magnified by about 2.5 times that for Fig. 3. The feature of eutectic mixtures is observed on a broad peak above the main peak. a) 22.6; b) 24.9; c) 26.5; d) 29.5 mol% mixtures

point. In order to clearly express a lower part of the peak front given in Fig. 3, the logarithm of the peak front is plotted against temperature (not reproduced here). Pure C39 and the mixture of $c = 22.6$ mol%, which is ascribed approximately to c_C, empirically give steep, straight lines, whereas the mixtures of the intermediate concentration show curvature. The temperature at which the DSC curve departs from the base line as indicated by a vertical bar in Fig. 3 was assigned as the initial melting point, which may correspond to the temperature of a solidus line. The temperature of a liquidus line was tentatively determined from a temperature at the point of inflection just before of the peak in the peak front, as is shown by an oblique line. This corresponds to the temperature at which the phase transition completes, according to the model calculation on heat-flux type DSC curves [13, 14]. The solidus and liquidus lines are drawn in Fig. 4. The fact that the temperatures defined above do not coincide at both ends, that is, at the pure C39 and the mixture at $c = 22.6$ mol%, could be ascribed to a kinetic factor in the DSC measurement. The phase diagram obtained is characteristic of the formation of a solid solution. On the other hand, the small peaks ascribed to the B and the C transition were observed on the range of the solid solution. It is interesting that the transition temperatures in the mixtures become higher with an increase in c, as shown in Fig. 4. This behavior is in contrast to that of the mixture of n-alkane homologues, where the transition temperature is lowered with adding homologues. The carbonyl groups seems to have an anchor effect, that is, to suppress the solid-solid transitions of n-alkanes by reducing the smearing effect of the potential along the chain axes [15, 16].

The DSC curves of the mixtures ($c \geq 22.6$ mol%) drawn in Fig. 5 clearly show the appearance of small peaks after the main melting peak. This phenomena may be interpreted as the result that the system changes to an eutectic mixture as in the case for K25/C26 system, which will be described in the next paragraph. The highest and the main peak temperatures are also plotted in Fig. 4. The value of c_C could be estimated as slightly larger than 22.6 mol% from this phase diagram. For the systems of Kn/Cn (n = 25, 29, and 31), the hexagonal transition was observed

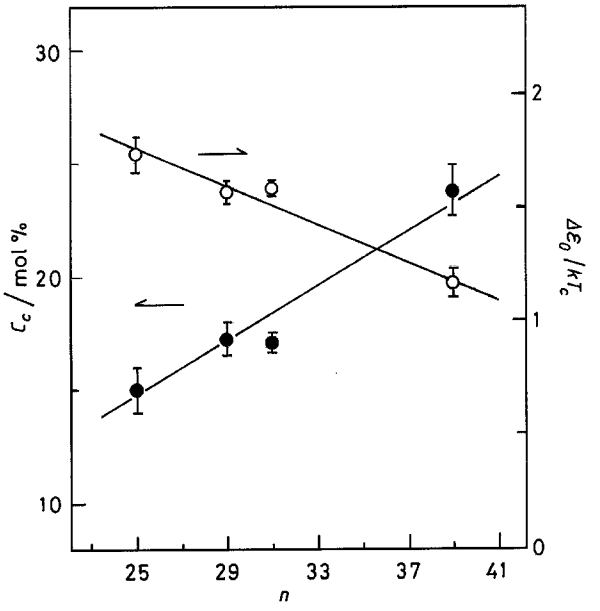

Fig. 6. Critical concentration (filled circles) and $\Delta\varepsilon_N/kT_c$ (open circles) for the systems of Kn/Cn (n = 25, 29, 31 and 39) vs. n (number of carbon atoms in a molecule)

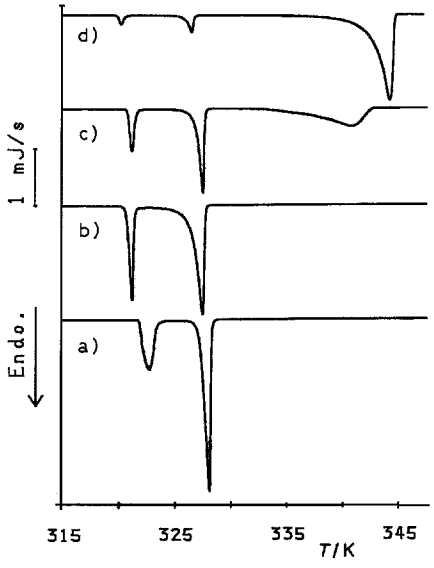

Fig. 7. DSC curves for the system of K25/C26. Mol % of ketone: a) 10.0; b) 20.0; c) 50.0; d) 90.0

over the whole concentration range. However, c_C could be similarly determined. The hexagonal transition temperature over the range of the solid solution was nearly independent of c or increased slightly with c. This is similar to the behavior of the B and the C transitions, as stated above.

For the system Kn/Cn, c_C and the $\Delta\varepsilon_0/kT_C$ calculated through Eq. (2) are plotted against n in Fig. 6. That $\Delta\varepsilon_0/kT_C$ decreases approximately linearly with n could be reasonably interpreted because the repulsive contribution of the carbonyl interactions per Kn molecule becomes smaller with an increasing n. The crystalline form at T_C does not seem to have a large effect on either quantities, because the relationships between both quantities and n are smooth.

The critical concentration for the systems of Kn/Cn′ ($n < n'$)

Figure 7 shows typical DSC curves of K25/C26 at various concentration. As stated in the preceding paragraph, the curves can be classified into two types, one for the solid solution and another for the eutectic mixture. Figure 8 shows DSC curves around c_C, which are magnified on the ordinate scale. On this short chain mixture, the

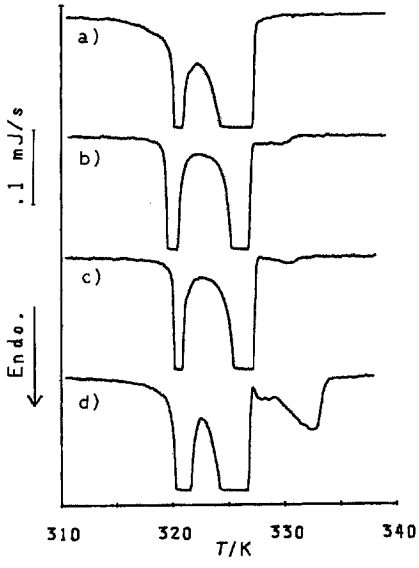

Fig. 8. DSC curves for the system of K25/26 around the critical concentration. The ordinate scale is magnified by about 17 times that for Fig. 7. Mol % of ketone: a) 23.0; b) 24.0; c) 25.0; d) 30.1

peak after the main peak can be easily detected (compare Fig. 5). The two regions of the mixture were, furthermore, confirmed by observation with the polarizing microscope. On the mixture ($c > c_C$), bright crystallites were observed in

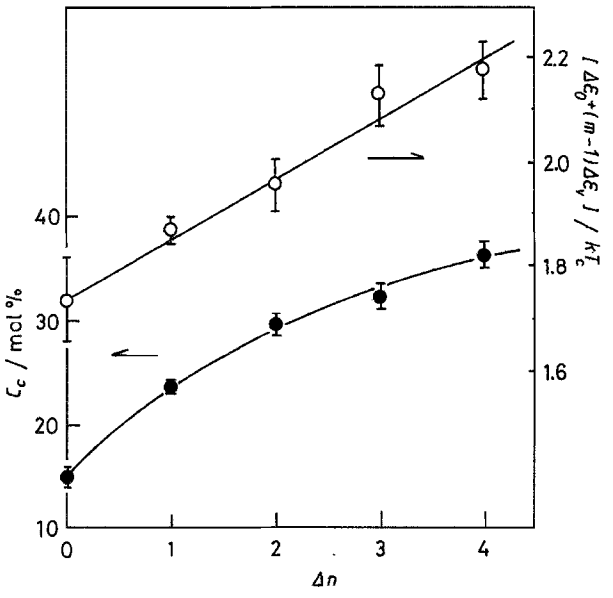

Fig. 9. Critical concentration (filled circles) and $[\Delta\varepsilon_0 + (m-1)\Delta\varepsilon_v]/kT_c$ (open circles) for the systems of K25/Cn (n = 25, 26, 27, 28, and 29) vs. the difference in n, Δn, which is equal to $m-1$

a dark liquid field at a temperature corresponding to the liquid-crystal's coexistence region of the phase diagram. On the other hand, on the mixture ($c < c_C$), the homogeneous textures were observed, which differed for the hexagonal and for the crystalline phase. These microscopic photographs were previously reported [17]. The crystalline form of the C26 matrix seems to change from the monoclinic to orthorhombic form with the increase of the concentration of K25. Because this change did not seem to affect the present discussion, the experimental confirmation was not performed.

In Fig. 9, c_C for K25/Cn (n = 25 ~ 29) is plotted by filled circles as a function of the difference in n, that is, $\Delta n = m - 1$. The remarkable increase of c_C with an increase of Δn could be ascribed to the first factor of m in the right-hand side of Eg. (4). The sum of the energy terms $[\Delta\varepsilon_0 + (m-1)\Delta\varepsilon_v]/kT_C$ is also plotted by open circles, where the additivity of both energies are apparently established. As previously stated, there is some possibility that $\Delta\varepsilon_0$ depends on m, and also $\Delta\varepsilon_v$ may differ at the position and the number of the vacant site. The apparent linear relationship suggests that either the effects stated above are not large or both terms of the energy compensate each other.

We can understand the increase in c_C for Kn/Cn′ ($n \leq n'$) in terms of the entropy of mixing given by Eq. (4), which is based on a very simple model. The present result indicates, furthermore, that the entropy of mixing plays an important role for the stability of the crystals composed of chain molecules. A more general case of this problem was discussed repeatedly by Mandelkern et al. [18, 19]. Their discussion has been based on Flory's model [20], where the melting point is a function of equilibrium crystallite thickness and surface energy. In the present treatment, the surface energy was assumed to be almost identical, irrespective of the kinds of the layered crystallites. This assumption might be reasonable because the comparison was done between the crystallites of different types. The multiplicity of the disposition along chain axes may correlate to the equilibrium crystallite thickness. The vacant sites energy in the present treatment may be partially included in the surface energy. The concept of the molecular segregation on crystallization from the melt, especially under high pressure, as it has been sometimes referred to [21], has to be examined from the view point of the effect of the entropy of mixing.

Lastly, we would like to comment on the phase diagram of K23/C26 reported by Meakins [6]. Although he gave c_C at low K23 concentration of about 5%, a value of $c_C \approx 31$ mol% was estimated from our relationships. This value approximately equals the concentration of the eutectic point of his diagram. His unappropriated assignment may come from his experimental technique.

Conclusion

The solubility limit of the solid solution for the systems of symmetrical long ketones in *n*-alkanes, Kn/Cn′ ($n \leq n'$), was determined with DSC measurements. For the case of n = n′ the relationship for the solubility limit (the critical concentration) of the solid solution was derived in terms of the position of Kn in the matrix and the substitutional energy. For the case of $n < n'$ the solubility limit increased with the increase in the difference between n′ and n. This was ascribed to the increase of the entropy of mixing owing to the

multiplicity of the positioning of Kn along Cn' despite of the increase in energy due to vacant sites. This result implies that the entropy of mixing plays an important role for the stability of crystals, even if the components are long-chain homologues, for example, *n*-alkanes.

Acknowledgement

This work was supported in part by a Grant-in Aid for Developmental Scientific Research (No. 03555191) from the Ministry of Education, Science and Culture of Japan.

References

1. Piesczek W, Strobl GR, Malzahn K (1978) Acta Crystallogr B30:1278
2. Takamizawa K, Ogawa Y, Oyama T (1982) Polym J 14:441
3. Takamizawa K, Urabe Y, Fujimoto J, Ogata H, Ogawa Y, unpublished work
4. Urabe Y, Takamizawa K (1992) Chem Lett 1877
5. Ewen B, Strobl GR, Richter D (1980) J Chem Soc Faraday Discuss 69:19
6. Meakins RJ (1949) Austral J Sci Res 2:405
7. Meakins RJ (1959) Trans Faraday Soc 55:1694
8. Meakins RJ (1959) Trans Faraday Soc 55:1702
9. Strobl GR, Trzebiatowski T, Ewen B (1978) Prog Colloid & Polym Sci 64:219
10. Asbach GI, Kilian HG, Stracke FR (1982) Colloid & Polym Sci 260:151
11. Takamizawa K, Sonoda T, Urabe Y (1989) Eng Sci Reports Kyushu Univ 10:363 (in Japanese)
12. Broadhurst MG (1962) J Res Natl Bur Std 66A:241
13. Mraw SC (1982) Rev Sci Instrum 53:228
14. Saito Y, Saito S, Atake T (1986) Thermochim Acta 99:299
15. Peterlin A, Fischer EW (1960) Z Physik 159:272
16. Peterlin A, Fischer EW, Reihold C (1962) J Chem Phys 37:1403
17. Takamizawa K, Nakasone K, Urabe Y, Sonoda T (1990) Eng Sci Reports Kyushu Univ 12:291
18. Mandelkern L, Stack GM (1984) Macromolecules 17:871
19. Mandelkern L, Prasad A, Alamo RG, Stack GM (1990) Macromolecules 23:3696
20. Flory PJ (1963) J Chem Phys 17:3548
21. Wunderlich B (1976) Macromolecular Physics Vol. 2 Crystal Nucleation, Growth, Annealing Chap. 5. Academic Press, New York

Received September 25, 1992;
accepted July 8, 1993

Authors' address:

Prof. Kanichiro Takamizawa
Department of Applied Science, Faculty of Engineering
Kyushu University
Hakozaki, Higashi-ku, Fukuoka 812, Japan